

Algorithmic Cooling in Liquid State NMR

Yosi Atia¹, Yuval Elias², Tal Mor³, Yossi Weinstein³

¹*School of Computer Science and Engineering, The Hebrew University, Jerusalem 91904, Israel*

²*Département IRO, Université de Montréal, Montréal (Québec) H3C 3J7, Canada and*

³*Computer Science Department, Technion, Haifa 320008, Israel*

Algorithmic cooling is a method that employs thermalization to increase qubit purification level, namely it reduces the qubit-system's entropy. We utilized gradient ascent pulse engineering (GRAPE), an optimal control algorithm, to implement algorithmic cooling in liquid state nuclear magnetic resonance. Various cooling algorithms were applied onto the three qubits of ¹³C₂-trichloroethylene, cooling the system beyond Shannon's entropy bound in several different ways. In particular, in one experiment a carbon qubit was cooled by a factor of 4.61. This work is a step towards potentially integrating tools of NMR quantum computing into in vivo magnetic resonance spectroscopy.

INTRODUCTION

The quantum computational model permits algorithms that provide significant — and sometimes even exponential — speed-up over any known classical counterpart [1–3]. A rather different scope of that model is to enable improved quantum technologies, e.g. quantum repeaters for communicating secure data over longer distances [4]. Algorithmic cooling, experimentally implemented in this work, is a method that might contribute to both scopes. On the one hand, it was originally suggested as a method for increasing the qubits' purification level [5–10], as qubits in a highly pure state are required both for initialization and for fault tolerant [11, 12] quantum computing. On the other hand, the suggested novel usage of data compression may potentially be found useful for increasing the signal to noise ratio of liquid-state NMR and in vivo magnetic resonance spectroscopy [6, 13, 14].

Nuclear magnetic resonance quantum computing (NMR-QC) [15–19] commonly uses spin 1/2 nuclei (hereinafter *spins*) of molecules as qubits. Compared to other implementations of small quantum computing devices, liquid-state NMR has an advantage of relatively easy realization of quantum gates by applying RF fields and utilizing spin-spin interactions. However, NMR-QC also has some disadvantages due to working with an ensemble of spins in a mixed state [20, 21], e.g. it is not scalable. Algorithmic cooling, in theory, resolves that problem [5–7].

The thermal energy at room temperature is much higher than the magnetic potential energy of nuclear spins even in the most advanced NMR devices. Therefore, at equilibrium, the qubit ensemble is in a highly mixed state - the probability difference between the “up” and “down” states (hereinafter the *polarization*, denoted as ε) is very small. At thermal equilibrium

$$\varepsilon = P_{\uparrow} - P_{\downarrow} = \tanh\left(\frac{\Delta E}{2k_B T}\right) \xrightarrow{\Delta E \ll k_B T} \frac{\Delta E}{2k_B T} = \frac{\hbar\gamma B_z}{2k_B T}. \quad (1)$$

Here γ is the gyromagnetic ratio of the spin, B_z is the intensity of the magnetic field, k_B is the Boltzmann constant and T is the bath temperature. When outside of equilibrium, spins with higher polarization than their thermal equilibrium polarization are considered “cool”, and we can use Eq. 1 to define the spin temperature as $T_{\text{spin}} = \frac{\hbar\gamma B_z}{2k_B \varepsilon}$.

Upper bounds on spin cooling (i.e. on polarization enhancement) can be derived by interpreting the spin state in terms of information theory [22]. The information content (*IC*) of the spin was defined using the conventional notion of Shannon entropy H . The relation between a single spin's polarization and *IC* is given by the following equation [23, 24]

$$H_{1\text{qubit}} = \left[\frac{1-\varepsilon}{2} \ln\left(\frac{1-\varepsilon}{2}\right) + \frac{1+\varepsilon}{2} \ln\left(\frac{1+\varepsilon}{2}\right) \right] \quad (2)$$

$$IC_{1\text{qubit}} = 1 - H_{1\text{qubit}} = \frac{\varepsilon^2}{\ln 4} + O(\varepsilon^4).$$

The information content of a spin system is invariant to reversible operations, and therefore bounds the maximal *IC* a single spin can reach by lossless manipulations, such as quantum gates. This entropy bound, also often called *Shannon's bound*, limits the maximal polarization of a single spin, given an initial thermal state of the spin system.

In our spin system, ¹³C₂-trichloroethylene (TCE, see Figure 1), consisting of a proton and two ¹³C, the *IC* at thermal equilibrium is:

$$IC_{eq} = \frac{\varepsilon_{H,eq}^2}{\ln 4} + 2 \frac{\varepsilon_{C,eq}^2}{\ln 4} = \left[\frac{\gamma_H^2}{\gamma_C^2} + 2 \right] \cdot \frac{\varepsilon_{C,eq}^2}{\ln 4} = 17.84 \frac{\varepsilon_{C,eq}^2}{\ln 4}. \quad (3)$$

Shannon's bound dictates that a single spin cannot hold more than the equilibrium information content of the entire spin system:

$$IC_{eq} = 17.84 \frac{\varepsilon_{C,eq}^2}{\ln 4} = \frac{\varepsilon_{max}^2}{\ln 4} \quad (4)$$

$$\Rightarrow \varepsilon_{max} = 4.224 \varepsilon_{C,eq}.$$

For convenience, we approximate $\gamma_H/\gamma_C = 4$, and then $\widetilde{IC}_{eq} = 18$, and $\widetilde{\varepsilon}_{max} = 4.24\varepsilon_{C,eq}$.

Algorithmic Cooling (AC) of spins counter-intuitively utilizes the heat bath, that decays polarizations to thermal equilibrium, to cool spins beyond Shannon's bound. AC requires a spin system where some spins, called *reset spins*, thermalize significantly faster than other spins, called *computation spins*. Reversible polarization compression (hereinafter *compression*) is applied to the spin system, transferring some of the computation spins' entropy to the reset spins, which quickly lose some of it to the environment. The process can be repeated, converging the system to a stable trajectory (limit-cycle) in the thermodynamic diagram. The efficiency and the cooling limit of AC are (ideally) dependent on the unitary restriction of processes between reset steps, and on the ratio between the relaxation times of the cooled spins and the reset spins.

Various cooling algorithms were developed, following the basic principle presented in [5]. For example, in a three qubit system with uniform equilibrium polarization ε , the initial information content is $IC_{eq} = 3\varepsilon^2/\ln 4$, the maximum polarization of a single spin that can be reached using unitary transformations [25, 26], is 1.5ε , and Shannon's bound for the maximal polarization of a single spin is $\sqrt{3}\varepsilon = 1.732\varepsilon$. But if one spin has a much shorter thermalization time than the other spins, it will reset while the others retain most of their polarization, so that the entire spin system is cooled. Ideally, iterating the compression process twice leads to a bias of 1.75ε , bypassing the result obtained by unitary transformations and even bypassing Shannon's bound [6]. Repeating the process while assuming infinite relaxation time ratios allows enhancing the polarization of one spin asymptotically to 2ε [27]. Algorithms applying these processes to n qubits ideally cool exponentially beyond the unitary cooling [5, 6], and can be practicable or optimal, see [6, 7, 24, 28–30].

In TCE, the proton reset spin has higher equilibrium polarization than C1 and C2, the ^{13}C computation spins. In such scenarios, even a special case — AC without compression (called heat bath cooling [14, 23]), can cool the spin system beyond Shannon's bound. This can be done by applying a polarization transfer [31] from the proton to C1, or alternatively, by swapping the two polarizations via a polarization exchange (PE) gate, and waiting for the proton to regain some of its polarization (while the carbon is still cool). A successive PE from the proton to C2 followed by another waiting period yields polarization of approximately 4 on all three spins, in units of carbon equilibrium polarization. If the relaxation time ratio is sufficiently large, and all gates are perfect then $\widetilde{IC}_{total} \rightarrow 48$, far above the initial approximate value of 18. Further cooling can be achieved using compression.

In practice, heat bath cooling of TCE [23], yielded polarizations $\{1.74, 1.86, 3.77\}$ for C1, C2 and the proton

respectively, well below the ideal $\{4, 4, 4\}$. Yet, the resulting total IC is $20.70 (\pm 0.06)$, which is beyond (and statistically significant) the experimental initial IC (of 17.84) at equilibrium, hence showing for the first time that the Shannon bound can be experimentally bypassed. Heat bath cooling on two amino-acids [14] also successfully bypassed Shannon's bound later on. On the other front, experimental work, cooling solely by compression was done by Sørensen [25] on methylene chloride, and by Chang, Vandersypen and Steffen [32] on three fluorines in $\text{C}_2\text{F}_3\text{Br}$. Full AC [33] and multi-cycle AC [34] using solid-state NMR was successfully done at the University of Waterloo.

MATERIALS AND METHODS

In order to implement AC and multiple-cycle AC on liquid-state TCE we utilized (following [34]) Gradient Ascent Pulse Engineering (GRAPE) [35], an optimal control algorithm, to generate high fidelity pulses for obtaining the compression gate and the PE gate [36]. Here we present various algorithms for cooling liquid TCE. Process 1 (see Figure 2), aimed to maximize IC_{C1} , is as follows:

1. Wait for duration D2 (H regains polarization)
2. PE(H \rightarrow C2)
3. Wait for duration D3 (H regains polarization)
4. Compression of C1, C2, H onto C1.
5. Return to step 1, unless C1 is saturated.

Ideally, the polarization of C1 saturated at $\widetilde{IC}_{C1} \rightarrow 64$. Process 2, aimed to maximize $IC_{C1,C2}$ is composed of Process 1 followed by a wait step for duration D4, and by PE(H \rightarrow C2) to cool C2, ideally reaching $\widetilde{IC}_{C1,C2} = 80$ (see Figure 3). The goal of Process 3 is to maximize IC_{total} , hence we apply Process 2, followed by a wait step for duration D5, ideally reaching $\widetilde{IC}_{total} = 96$ (see Figure 4). In all cases, a read-out pulse was applied on the spin of interest prior to acquisition.

In the experiment, the measured relaxation times (see table I), were obtained by inversion recovery as in [23, 36]. Adding a paramagnetic reagent to the TCE, improved the relaxation time ratios as suggested in [37]. We simulated the three processes using the experimental delays and measured relaxation times, while assuming perfect pulses. According to the simulation, the polarization of C1 could be enhanced by a factor of 5.49 after seven rounds ($IC_{C1} = 30.13$, see also Figure 6) via Process 1, the polarization of the two carbon spins could reach 4.78 and 3.70 ($IC_{C1,C2} = 36.53$) via Process 2. The polarization of three spins could reach $\{3.98, 2.97, 3.75\}$ ($IC = 38.73$) via Process 3.

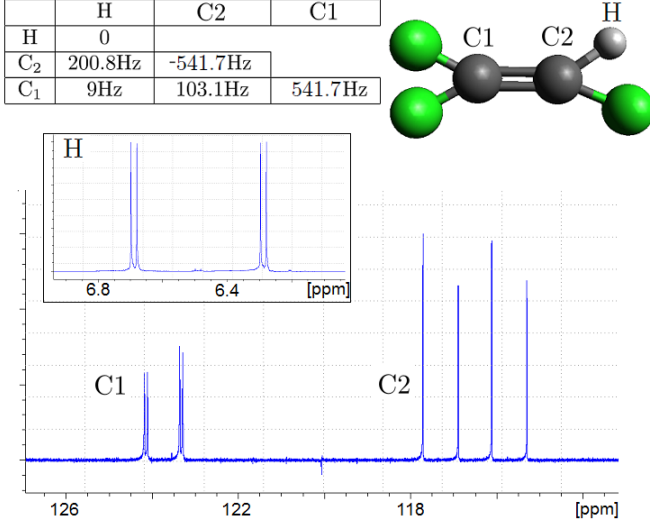


FIG. 1: (Color online) $^{13}\text{C}_2\text{-TCE}$ with paramagnetic reagent $\text{Cr}(\text{acac})_3$, in CDCl_3 (chloroform-d) solution. The experiments were performed on a Bruker Avance III 600 spectrometer using a standard 5 mm double resonance probe with a broadband inner coil tuned to ^{13}C and an outer ^1H coil probe. This sample has three active spins marked H, C2, and C1. In the table, the chemical shifts relative to the transmitter frequency are in the diagonal cells, and the J-couplings are in the off-diagonal cells. The carbon spectrum is at the bottom, the proton spectrum is in the small frame. The units of the x axis are parts-per-million.

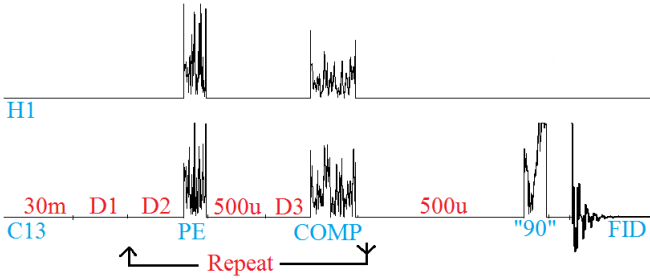


FIG. 2: (Color online) Visualization of Process 1, based on the TopSpin[®] output, showing the RF power vs time in both channels, followed by an acquisition of the free induction decay (FID). The PE and COMP pulses are 6.5 msec and 13 msec long respectively, and the delays maximizing the polarization of C1 are $D_2=5\text{s}$, $D_3=3\text{s}$. The delay D_1 was set to 150s to equilibrate the system.

The implemented PE and compression pulses were generated using SIMPSON version 3.0 [38, 39], an open source program implementing GRAPE. The pulses were designed to be robust to deviations up to $\pm 15\%$ in RF power [36]. The pulses were not designed to apply a spe-

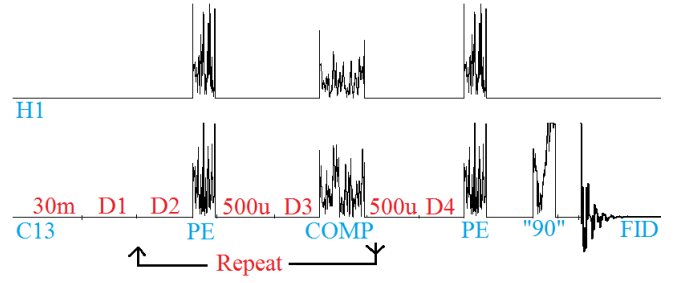


FIG. 3: (Color online) Visualization of Process 2, based on the TopSpin[®] output, showing the RF power vs time in both channels, followed by an acquisition of the free induction decay (FID). The delays maximizing the polarization of C1 are $D_2=5\text{s}$, $D_3=3\text{s}$, and $D_4=5\text{s}$.

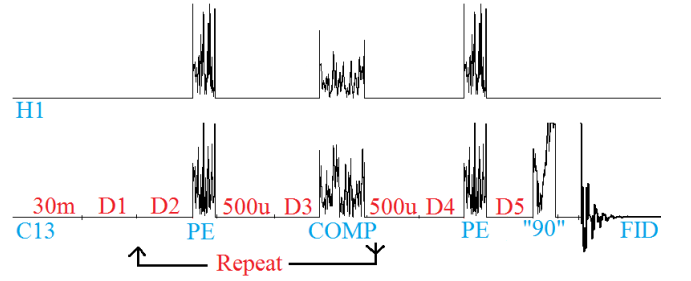


FIG. 4: (Color online) Visualization of Process 3, based on the TopSpin[®] output, showing the RF power vs time in both channels, followed by an acquisition of the free induction decay (FID). The delays maximizing the polarization of C1 are $D_2=5\text{s}$, $D_3=3\text{s}$, $D_4=6\text{s}$, and $D_5=6\text{s}$.

cific unitary gate, but to apply a less constraining state-to-state transformation. However the state of the system changes with each cooling cycle. Therefore, among two pulses that apply PE, even though one pulse performs better in equilibrium [36], we used another pulse, which yielded better cooling for the entire process. Let $\{\{\dots\}\}$ stand for the diagonal of a density matrix in the computation basis. The PE pulse was designed to evolve the system from equilibrium

$$4I_z^H + I_z^{C2} + I_z^{C1} \propto \{\{6, 4, 4, 2, -2, -4, -4, -6\}\}, \quad (5)$$

to a finite state,

$$I_z^H + 4I_z^{C2} + I_z^{C1} \propto \{\{6, 4, -2, -4, 4, 2, -4, -6\}\}, \quad (6)$$

where $I_z = \frac{1}{2}\sigma_z$. The two states are represented here [40] in product operator formalism as the reduced (shifted and scaled [28]) diagonal density operator [15, 36]. The compression pulse (COMP) was designed to evolve the system from

$$I_z^H + I_z^{C2} + I_z^{C1} \propto \{\{3, 1, 1, -1, 1, -1, -1, -3\}\} \quad (7)$$

TABLE I: Measured relaxation times of TCE in units of seconds.

	H	C2	C1
T_1	2.67 ± 0.03	17.3 ± 0.2	29.2 ± 0.1
T_2^*	0.2 ± 0.01	0.44 ± 0.03	0.23 ± 0.01

(a state of three spins with identical polarizations) to

$$\frac{1}{2}I_z^H + \frac{1}{2}I_z^{C2} + \frac{3}{2}I_z^{C1} + 2I_z^H I_z^{C2} I_z^{C1} \propto \{3, 1, 1, 1, -1, -1, -1, -3\}. \quad (8)$$

We chose this final state, as the four highest probabilities correspond to the four states where C1's spin is 0, namely, $|0ij\rangle, ij \in 0, 1$. Notice that the polarization-increase factor of C1 is 1.5, the maximum possible under unitary transformations, as mentioned above.

RESULTS

After seven rounds (see Figure 6), the system reached its limit cycle and no more improvement could be expected. In Process 1, C1 was cooled by a factor of 4.61 ± 0.02 , with $IC_{C1} = 21.25 \pm 0.18$, significantly higher than 17.84, the IC of the entire spin system at equilibrium (see Figures 6 and 5). Alternatively, we see that the polarization bypassed the information theoretical bound of $\sqrt{17.84} = 4.22$. In Process 2 we maximized $IC_{C1,C2}$, by adding another delay, D4 (that happened to be equal to D2=5s in the optimal case), followed by PE. We obtained polarizations of 3.78 ± 0.02 and 3.4 ± 0.02 (of C1 and C2 respectively), with $IC_{C1,C2} = 25.9 \pm 0.2$. In Process 3 we maximized the total IC , using an additional delay D5=6s before the measurement (in addition, D4 was modified to 6s). The measured polarizations were 2.87 ± 0.02 , 2.64 ± 0.02 and 3.58 ± 0.02 (for C1, C2, and H respectively), with IC of 28.0 ± 0.20 .

There is a gap between SIMPSON's very high predicted pulse efficiency and the lab results (see [36]). The polarization of C2 following a PE pulse was ≈ 3.8 (0.95 efficiency), and a COMP pulse applied on equilibrium state resulted with $\varepsilon_{C1} \approx 2.8$ (0.92 efficiency). The main error factors are the hardware's imperfection distorting the pulses [41], and the pulses themselves being prepared without taking into account the T_2^* -relaxation (see table I) during the system evolution. The first factor could be negated using a technique mentioned in [34]. Once the measured gate-efficiencies of 0.95 and 0.92 are added into the simulation, the simulated IC per round fit near-perfectly the measured IC , see Figures 6 and 7.

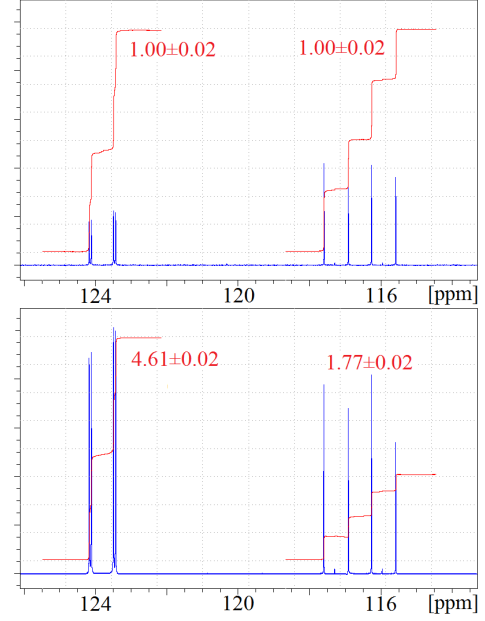


FIG. 5: (Color) the ^{13}C carbon spectrum before and after seven cycles of algorithmic cooling to maximize the polarization of C1. The peak integrals are displayed in red (arbitrary units).

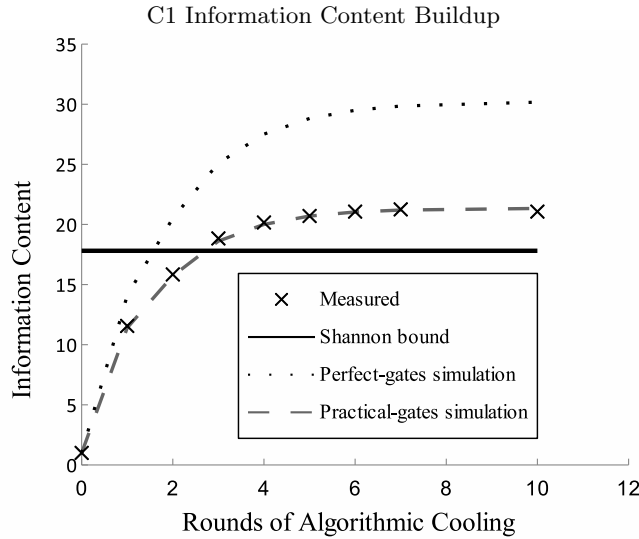
SUMMARY

Using optimal control, we demonstrated the first single-round and multiple round AC applied on liquid state NMR. We bypassed Shannon's bound in three different processes. The current optimal control methods (GRAPE), and better ones such as a second order GRAPE [42] and Krotov based optimization [43] could enable various applications of AC in magnetic resonance spectroscopy [13, 14, 44] and maybe also other potential applications [45–54].

ACKNOWLEDGMENTS

We thank Prof. Asher Schmidt and Dr. Yael Balasz for enlightening discussions. This work was supported in part by the Wolfson Foundation and the Israeli MOD Research and Technology Unit. YE thanks the Institut Transdisciplinaire d'Information Quantique.

-
- [1] D. Simon, in *Foundations of Computer Science, 1994 Proceedings., 35th Annual Symposium on the Foundations of Computer Science* (1994), pp. 116–123.
 - [2] P. W. Shor, *SIAM J. Comp.* **26**, 1484 (1997).
 - [3] A. W. Harrow, A. Hassidim, and S. Lloyd, *Phys. Rev. Lett.* **103**, 150502 (2009).



Round	Polarization	Carbon's IC
0	1.00	1.00 ± 0.04
1	3.40	11.56 ± 0.14
2	3.98	15.84 ± 0.16
3	4.34	18.84 ± 0.17
4	4.49	20.16 ± 0.18
5	4.55	20.70 ± 0.18
6	4.59	21.07 ± 0.18
7	4.61	21.25 ± 0.18
10	4.59	21.07 ± 0.18

FIG. 6: On the left, the measured IC vs the simulated IC of C1 at each cooling round of Process 1, in units of $\frac{\varepsilon_{C,eq}^2}{\ln(4)}$ (see [23]), where $\varepsilon_{C,eq}$ is the carbons' equilibrium polarization. On the right, the measured polarization and IC of C1 in each round. The measured error of all the polarizations is 0.02.

- [4] H.-J. Briegel, W. Dür, J. I. Cirac, and P. Zoller, Phys. Rev. Lett. **81**, 5932 (1998).
- [5] P. O. Boykin, T. Mor, V. Roychowdhury, F. Vatan, and R. Vrijen, Proc. Natl. Acad. Sci. USA **99**, 3388 (2002).
- [6] J. M. Fernandez, S. Lloyd, T. Mor, and V. Roychowdhury, Int. J. Quant. Inf. **2**, 461 (2004).
- [7] L. J. Schulman, T. Mor, and Y. Weinstein, Phys. Rev. Lett. **94**, 120501 (2005).
- [8] S. Raesi and M. Mosca, Phys. Rev. Lett. **114**, 100404 (2015).
- [9] N. A. Rodriguez-Briones and R. Laflamme, arXiv:1412.6637 (2015).
- [10] D. K. Park, N. A. Rodriguez-Briones, G. Feng, R. Rahimi-Darabad, J. Baugh, and R. Laflamme, arXiv:1501.00952 (2015).
- [11] E. Knill, R. Laflamme, and W. H. Zurek, Proc. Roy. Soc. London, Ser. A **454**, 365 (1998).
- [12] D. Aharonov and M. Ben-Or, in *Proc. 29th STOC* (ACM, 1997), pp. 176–188.
- [13] T. Mor, V. Roychowdhury, S. Lloyd, J. M. Fernandez, and Y. Weinstein, *US patent No. 6,873,154* (2005).
- [14] Y. Elias, H. Gilboa, T. Mor, and Y. Weinstein, Chem. Phys. Lett. **517**, 126 (2011).
- [15] D. G. Cory, A. F. Fahmy, and T. F. Havel, in *Proceedings of the Fourth Workshop on Physics and Computation* (1996), pp. 87–91.
- [16] D. G. Cory, R. Laflamme, E. Knill, L. Viola, T. F. Havel, N. Boulant, G. Boutis, E. Fortunato, S. Lloyd, R. Martinez, et al., Fortschr. Phys. **48**, 875 (2000).
- [17] S. J. Glaser, Angewandte Chemie **40**, 147 (2001).
- [18] L. M. K. Vandersypen and I. L. Chuang, Rev. Mod. Phys. **76**, 1037 (2005).
- [19] J. A. Jones, Prog. NMR Spectrosc. **59**, 91 (2011).
- [20] N. A. Gershenfeld and I. L. Chuang, Science **275**, 350 (1997), URL <http://citeseer.nj.nec.com/gershenfeld97bulk.html>.
- [21] P. O. Boykin, T. Mor, V. Roychowdhury, and F. Vatan, Nat. Comp. **9**, 329 (2010).
- [22] T. Cover and J. Thomas, *Elements of Information Theory*, Wiley Series in Telecommunications and Signal Processing (Wiley-Interscience, 2006), ISBN 9780471241959.
- [23] G. Brassard, Y. Elias, J. M. Fernandez, H. Gilboa, J. A. Jones, T. Mor, Y. Weinstein, and L. Xiao, arxiv:quant-ph/0511156 (2005), arXiv:quant-ph/0511156.
- [24] Y. Elias, J. M. Fernandez, T. Mor, and Y. Weinstein, in *Proceedings of Unconventional Computation* (Springer publishing, 2007), vol. 4618, pp. 2–26.
- [25] O. W. Sørensen, Prog. Nucl. Mag. Res. Spec. **21**, 503 (1989).
- [26] L. J. Schulman and U. V. Vazirani, in *ACM Symposium on the Theory of Computing (STOC): Proceedings* (1999), pp. 322–329.
- [27] J. M. Fernandez, Ph.D. thesis, University of Montreal, Canada (2003).
- [28] Y. Elias, J. M. Fernandez, T. Mor, and Y. Weinstein, Isr. J. Chem. **46**, 371 (2006).
- [29] L. J. Schulman, T. Mor, and Y. Weinstein, SIAM J. Comp. **36**, 1729 (2007).
- [30] Y. Elias, T. Mor, and Y. Weinstein, Phys. Rev. A **83**, 042340 (2011).
- [31] G. A. Morris and R. Freeman, J. Am. Chem. Soc. **101**, 760 (1979).
- [32] D. E. Chang, L. M. Vandersypen, and M. Steffen, Chem. Phys. Lett. **338**, 337 (2001).
- [33] J. Baugh, O. Moussa, C. A. Ryan, A. Nayak, and R. Laflamme, Nature **438**, 470 (2005).
- [34] C. A. Ryan, O. Moussa, J. Baugh, and R. Laflamme, Phys. Rev. Lett. **100**, 140501 (2008).
- [35] N. Khaneja, T. Reiss, C. Kehlet, T. Schulte-Herbrüggen, and S. J. Glaser, J. Mag. Reson. **172**, 296 (2005).
- [36] Y. Atia, Y. Elias, T. Mor, and Y. Weinstein, Int. J. Quant. Inf. **12**, 1450031 (2014).

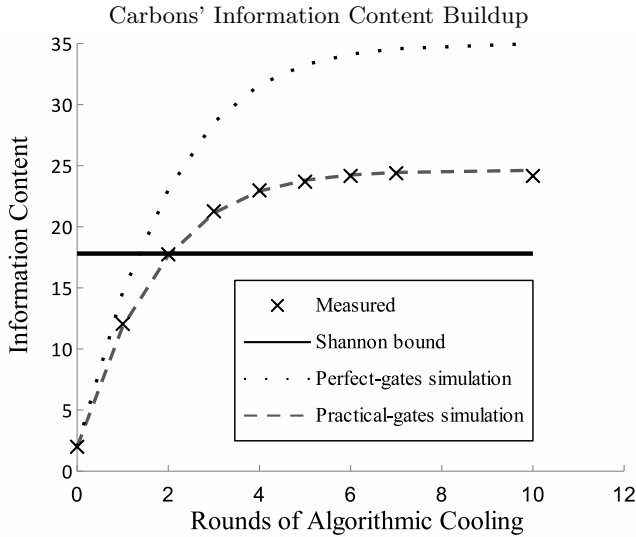


FIG. 7: The carbons' information content at each cooling round of Process 2 in units of $\frac{\varepsilon_{C,eq}^2}{\ln(4)}$ (see [23]), where $\varepsilon_{C,eq}$ is the equilibrium polarization of the carbons. The measured error of all polarizations is 0.02.

- [37] J. M. Fernandez, T. Mor, and Y. Weinstein, *Int. J. Quant. Inf.* **3**, 283 (2005).
- [38] M. Bak, J. T. Rasmussen, and N. C. Nielsen, *J. Mag. Reson.* **147**, 296 (2000), ISSN 1090-7807.

- [39] Z. Tošner, T. Vosegaard, C. Kehlet, N. Khaneja, S. Glaser, and N. Nielsen, *J. Mag. Reson.* (2008).
- [40] Note1, in the actual design we used the more precise γ ratio of 3.98, but in the explanation here we use 4 for clarity.
- [41] T. M. Barbara, J. F. Martin, and J. G. Wurl, *Journal of Magnetic Resonance* (1969) **93**, 497 (1991).
- [42] P. de Fouquieres, S. Schirmer, S. Glaser, and I. Kuprov, *J. Mag. Reson.* **212**, 412 (2011).
- [43] I. I. Maximov, Z. Tošner, and N. C. Nielsen, *J. Chem. Phys.* **128**, 184505 (2008).
- [44] G. Brassard, Y. Elias, T. Mor, and Y. Weinstein, *Eur. Phys. J. Plus* **129**, 258 (2014).
- [45] F. Rempp, M. Michel, and G. Mahler, *Phys. Rev. A* **76**, 032325 (2007).
- [46] M. J. Henrich, F. Rempp, and G. Mahler, *Eur. Phys. J. Spec. Top.* **151**, 157 (2007).
- [47] H. Weimer, M. J. Henrich, F. Rempp, H. Schröder, and G. Mahler, *Europhys. Lett.* **83**, 30008 (2008).
- [48] H. J. Briegel and S. Popescu, *arxiv:0806.4552* (2008), arXiv:0806.4552.
- [49] N. Linden, S. Popescu, and P. Skrzypczyk, *Phys. Rev. Lett.* **105**, 130401 (2010).
- [50] B. Criger, O. Moussa, and R. Laflamme, *arxiv:1103.4396* (2011), arxiv:1103.4396.
- [51] R. Renner, *Nature* **482**, 164 (2012).
- [52] A. Blank, *Quantum Inf. Processing* **12**, 2993 (2013).
- [53] J.-S. Xu, M.-H. Yung, X.-Y. Xu, S. Boixo, Z.-W. Zhou, C.-F. Li, A. Aspuru-Guzik, and G.-C. Guo, *Nat. Photonics* **8**, 113 (2014).
- [54] S. Lloyd, *Nat. Photonics* **8**, 90 (2014).